View metadata, citation and similar papers at core.ac.uk

brought to you by CORE

provided by IntechOpen

We are IntechOpen, the world's leading publisher of Open Access books Built by scientists, for scientists

4,800
Open access books available

122,000
International authors and editors

135M
Downloads

Our authors are among the

154
Countries delivered to

TOP 1%
most cited scientists

12.2%
Contributors from top 500 universities

CLARIVATE ANALYTICS BOOK CITATION INDEX INDEXED

WEB OF SCIENCE™

Selection of our books indexed in the Book Citation Index in Web of Science™ Core Collection (BKCI)

Interested in publishing with us?
Contact book.department@intechopen.com

Numbers displayed above are based on latest data collected.
For more information visit www.intechopen.com

9

Fuzzy Maximum Power Point Tracking Techniques Applied to a Grid-Connected Photovoltaic System

Neson Diaz, Johann Hernández, Oscar Duarte
Universidad Nacional, División de Investigación Bogotá, LIFAE, Universidad Distrital F.J.C.
Colombia

1. Introduction

Issues such as the increasing worried about global warming caused by the use of energy resources based on fossil fuel such as oil, gas and coal, have pointed the target toward sustainable energy resources free of greenhouse gas emissions. The PhotoVoltaic (PV) energy plays an important role into the called green energies sources, reason why its use has been rapidly invigorated A. Yafaoui (2009). However of this, a PV generator has two significant problems; the mismatch between the load and the conductance of the PV generator . Since, the load must match PV conductance of the PV generator to ensure the maximum power transfer A. Yafaoui (2009), Hohm & Ropp (2000). The other point, is that the PV generation depends of the weather conditions, such as solar irradiance and temperature Mutoh et al. (2006).

To ensure the maximum power transfer the load seen from the PV generator must be continuously adjusted. Therefore, a Maximum Power Point Tracking (MPPT) algorithm must be implemented to achieve the match between the PV generator (PVG) and the load in real time, taking into account that the maximum power point is not known a priori it is not an easy task to track the maximum power point Mutoh et al. (2006) Kim et al. (2006), Zeng & Liu (2009). Additionally, regarding the low efficiency of a PVG it would be desirable to obtain the maximum power under any weather condition Mutoh et al. (2006), Roman et al. (2006).

Many MPPT algorithm methods have been proposed to deal with the problem of the power generation variations due to changes at the solar irradiance and at PV cell temperature. They range from simple algorithm based on perturbation and observation to more complex based on neural network, and fuzzy logic control A. Yafaoui (2009), Hohm & Ropp (2000), Zeng & Liu (2009).

A PV system can be implemented as a stand-alone system or as a grid connected generator. A stand-alone system requires a battery bank to store the energy obtained from the PV generator. That kind of system is frequently used in low power system to support a local energy requirement. On the other hand, a grid-connected PV system (GCPVS) usually does not require the battery bank and has become the primary method for high-power applications Kim et al. (2006). A GCPVS takes an important part into distributed power generation systems such as low-voltage distribution grids Alonso-Martinez et al. (2009), Vandoorn et al. (2009), Xue et al. (2004). Where, the energy generated by the GCPVS is sent to the power grid and consumed by the nearest customers. This is accomplished through an efficient DC/AC conversion by means of a solid-state Inverter. The inverter becomes the interface between the

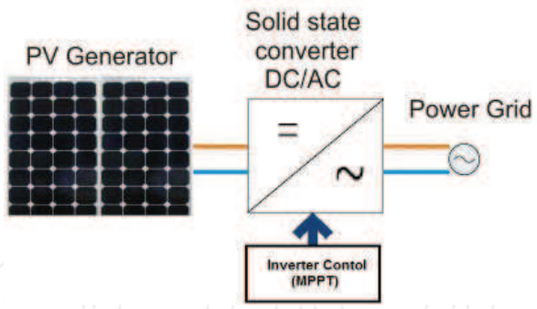

Fig. 1. Grid-Connected Photovoltaic System schematic.

AC grid load and the PVG, it has to match the PVG output resistance to ensure the MPPT (active power flow control).
In this chapter, a controller for a solid state inverter in a single phase GCPVS is proposed looking for MPPT. First the components of the GCPVS are explorer and the nonlinear current-Power relationship of a PVG is analyzed. Second a MPPT algorithm based on fuzzy logic is proposed and improved by means a short circuit current estimator based on a TakagiSugeno (TS) fuzzy model BABUSKA (2009). Third simpler linear controllers are used to achieve the maximum power point where the reference is imposed by the short circuit current estimator. The controllers were verified in simulation under various weather conditions.

2. Proposed grid connected photovoltaic system

A typical GCPVS as shown in figure 1 is composed by the PV modules, a Solid-state DC/AC conversion stage which is the interface between the variable DC generator and the power grid. For instance, at this case of study, the system will supply power to a single power grid $V_s = 120V \overset{to}{\rightarrow} 60Hz$. The conversion stage can be composed by a single o dual power processing stage Xue et al. (2004), Kjaer et al. (2005). Moreover, the conversion stage must also include a MPPT algorithm in order to obtain the maximum power generated from the PVG Kjaer et al. (2002). Next follows a brief analysis and description for each CGPVS component.

2.1 PV generator

By means of a p-n semiconductor junction it is possible to convert the solar radiation into DC currents using the photovoltaic effect. A PV panel is composed by an array of PV cells grouped together in series to increase the output voltage (usually 12 or 24 V), or in parallel to increase the electrical current that the PV module can provide to the load Kim et al. (2006), Molina & Mercado (2008). The traditional equivalent circuit of a solar cell is build by a photocurrent source I_{ph}, a diode parallel to the source, a series resistor R_s, and a shunt resistor R_{sh} as shown in figure 2 Kim et al. (2006), Xiao et al. (2006). A PV panel is composed by an array of cells, then an equivalent circuit for the PV module has the same configuration. Hence, the model of a single cell can be extrapolated to a PV panel model and consequently to a PV panels array interconnected in serial or parallel configuration. The equivalent circuit shown in figure 2, is useful to obtain a model of the PVG to simulate the system under different weather conditions Mutoh et al. (2006), Kim et al. (2006).
From the circuit in figure 2 the output current I is expressed by Mutoh et al. (2006):

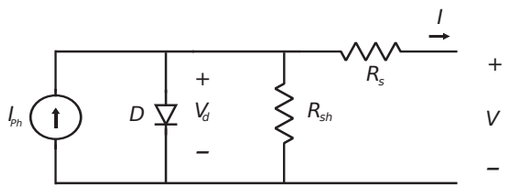

Fig. 2. Equivalent circuit of a PV generator.

$$I = I_{ph} - I_0 \left[exp^{\left(\frac{V+IR_s}{V_t}\right)} - 1 \right] - (V + IR_s)/R_{sh} \quad (1)$$

Where:

- $V_t = \frac{nKT}{q}$;
- n is the diode factor (ideality factor $(=1)$ maximum value 2) Mutoh et al. (2006),Kim et al. (2006);
- I_O cell reverse saturation current;
- K Boltzmanns constant $(= 1.38x10^{-23} Nm/K)$;
- T cell temperature (in kelvin);
- q electronic charge$(= 1.6x10^{-19} C)$;
- I Output current (A).
- V Output voltage (V).

The two internal resistances R_s and R_{sh} are usually neglected in order to simplify the model Mutoh et al. (2006), Kjaer et al. (2005). Hence, (1) is simplified to:

$$I = I_{ph} - I_0 \left[exp^{\left(\frac{V}{V_t}\right)} - 1 \right] \quad (2)$$

However, it is not an easy task for the users to obtain further information about n and I_0. Generally Those parameters are not listed in data sheets. Instead of those parameters in data sheets are listed the short-circuit current I_{sc} and the open circuit voltage V_{oc} under standard irradiance conditions $(1000W/m^2$ at 25^oC in a cell) Mutoh et al. (2006). Furthermore, the following expression can be used.

$$I_{sc} = I_{ph} \ (V = 0,\ I = I_{sc}) \quad (3)$$

$$I_0 = I_{sc} exp^{\left(-\frac{V_{oc}}{V_t}\right)}; (I = 0,\ V = V_{oc}) \quad (4)$$

The maximum power generated by the PV panel is also specified in the data sheet. That power is written in terms of the Current I_{pm} and Voltage V_{pm} at maximum-power point. Those parameters have been measured under standard condition. From (2) to (4) regarding that $exp^{\left(\frac{V+IR_s}{V_t}\right)} > 1$ under normal operation of the diode, the following expressions can be approximated as Mutoh et al. (2006):

$$I_{pm} = I_{sc}\left[1 - exp^{\left(\frac{V_{pm}-V_{oc}}{V_t}\right)}\right] \tag{5}$$

$$\frac{1}{V_t} = \frac{1}{(V_{pm} - V_{oc})}\log\left(1 - \frac{I_{pm}}{I_{sc}}\right) \tag{6}$$

Thus V_t and hence n can be obtained from (6). The output voltage of the PV generator can be expressed as a function of the output current, using parameters such as V_{oc}, I_{sc}.

$$V = V_{oc}\left\{1 + V_t \log\left(1 - \frac{I}{I_{sc}}\right)\right\} \tag{7}$$

(7) can be used as the model of the PVG. The power generated from the PV array is:

$$P = I * V = I * V_{oc}\left\{1 + V_t \log\left(1 - \frac{I}{I_{sc}}\right)\right\} \tag{8}$$

Other important parameters provided by the manufacturer are the Cell temperature coefficients, those parameters provide information about how the electrical parameters could vary under temperature change. In the table 1 are summarized the main electrical data provided by the manufacturer under standard condition. In this case for the study as PVG are used two panels ASE-300-DGF/17, with a nominal power of 300W each one. The two panels are connected in series hence the PV generator can provide a nominal power of 600W. The Open-circuit voltage temperature coefficient $T_K(V_{oc})$, and the value of n obtained from (6) are also summarized at the table 1.
The data reported in table 1 are used in the expression (7) to obtain the I-V curve under SIC; however, it would be desirable to obtain the I-V curve under different weather conditions. Taking into account the expression (3), there is also a proportional relationship between the short-circuit current I_{sc} and the solar irradiance Mutoh et al. (2006). Hence, by assuming that the I_{sc} change in the same proportion than the solar irradiance, it is possible to obtain the I-V curve under different weather conditions as is shown in fig 3. Figure 4 shows P-I curves under different weather conditions obtained from (8).

	PV panel	PV generator
P_{max} (Watts)	300 W	600 W
V_{pm}	17.2 V	34.4 V
I_{pm}	17.4 A	17.4 A
V_{oc}	20 V	40 V
I_{sc}	19.1 A	19.1 A
$T_K(V_{oc})$	$-0.38\%/C$	$-0.38\%/C$
n	1.6311	1.6311

Table 1. Data PV panel and PV generator

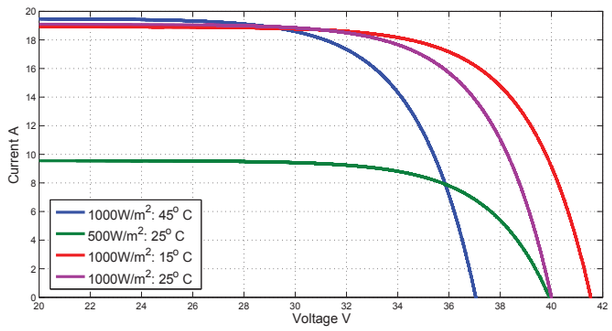

Fig. 3. I-V Curve under different environmental conditions.

2.2 Inverter

The main function of an inverter is to convert the DC voltage obtained from the PV generator into an AC current. Besides, it is the interface between the variable DC generator and the power grid. The inverter involves three major tasks; Inject sinusoidal current into the power grid; provide compensation against harmonic and reactive power; and finally the inverter must ensure maximum power tracking (MPPT) Kjaer et al. (2005), Patel & Agarwal (2006).
A dual-stage inverter have been selected for the GCPVS like the shown in figure 5, it offers an additional degree of freedom in the operation of the system than the one-stage configuration Xue et al. (2004), Kjaer et al. (2005). Instead of the degree of freedom, it is decreased global efficiency of the inverter because of the connection of two converters.
The first stage is a DC- DC boost converter that boosts and regulates the voltage V_{dc}, advisable for a normal operation of the inverters since it requires that $V_{dc} > V_s$ in spite of disturbances (the PV voltage vary in a wide range) Zhang & Xu (2001). The output voltage is a function of the input voltage, the duty cycle D (period of time in witch the MOSFET Q_1 in figure 5 is active), the load current as well as the values of converter components. Neglecting losses the output voltage of the boost converter is given by the equation (9) Erickson & Maksimovic (2000).

$$V_{dc} = \frac{V}{(1-D)} \tag{9}$$

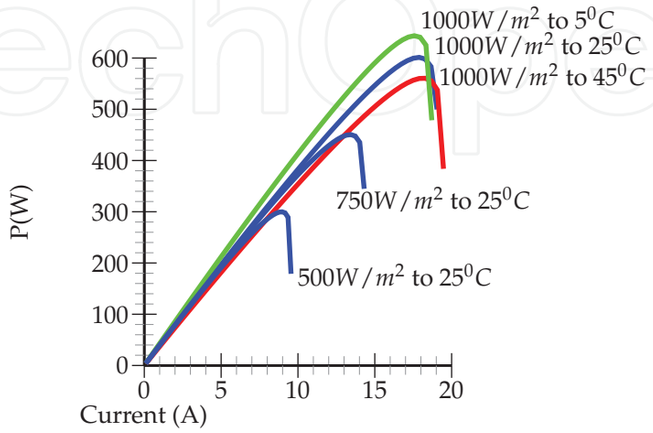

Fig. 4. P-I curves.

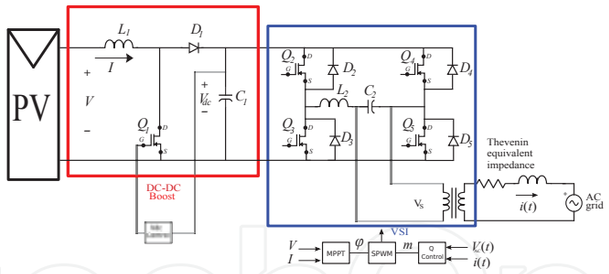

Fig. 5. Two-stage boost inverter Xue et al. (2004).

At this case the boost converter has been dimensioned for an output voltage $Vdc = 70V$. Hence, a compensator has been designed regarding the worst phase margin obtained from load variations and input voltage variations, to attain adequate phase margin and good rejection of expected disturbances. The compensator design was developed by frequency domain response. In figure 6 is shown the frequency response of the compensated loop gain $T(S)$ and the sensitivity function $1/(1+T(S))$ Erickson & Maksimovic (2000). The compensator design will not be explored in deep at this chapter, because of, it is out of the scope of this Chapter.

The second stage, a voltage-source inverter (VSI), converts the regulate DC voltage V_{dc} into an AC current. The inverter becomes the load seen from the first stage. Hence, the VSI operation point is adjusted to perform the MPPT. A sinusoidal AC voltage $v_c(t)$ as shown in (10) can be virtually generated at any angle and amplitude using Sinusoidal Pulse Wide Modulation (SPWM) techniques at forced commutation and subsequent filtering of high frequency components. The active and reactive power flow can be independently controlled manipulating the phase and amplitude of the AC wave voltage generated by the converter Sood (2004), Diaz et al. (2007), Zhang & Xu (2001), Gengyin et al. (2004), Padiyar & Prabhu (2004). This assumption is based on the fact that the VSI connected to an active AC grid behaves like the stator of a synchronous machine (figure 7), regarding only the fundamental frequency component. The active and reactive power flow neglecting the losses are given by (11) and (12), Diaz et al. (2007), Ruihua et al. (2005), Li et al. (2006). In (11) and (12) V_c is the fundamental component of the converter voltage, V_s is the fundamental component of the AC grid voltage, X is the reactance of the reactor that connects the two voltage sources, φ is the phase shift between V_c and V_s. At figure 7, r represents the losses at the conversion stage. In order to simplify the analysis r is neglected; this assumption can be done taking into account that typically the VSI losses are usually less than 5% of the rated capacity Diaz et al. (2007),

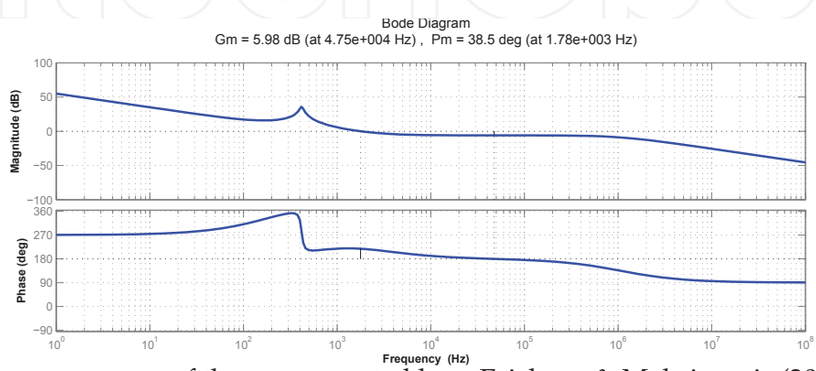

Fig. 6. Frequency response of the compensated loop Erickson & Maksimovic (2000).

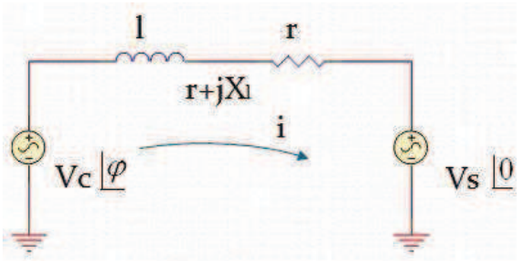

Fig. 7. Equivalent circuit of a VSI interconnected to the AC grid.

Zhang & Xu (2001).

$$v_c(t) = mV_{dc}\sin(\omega t + \varphi) \tag{10}$$

$$P = \frac{V_c V_s}{X}\sin(\varphi) \tag{11}$$

$$Q = \frac{V_s(V_s - V_c\cos(\varphi))}{X} \tag{12}$$

(11) and (12) show that P depends mainly of the angle φ and Q depends mainly of V_c amplitude, which is controlled by the modulation ratio m that is the relationship between the peak AC output voltage and the DC voltage $m = V_{c(peak)}/V_{dc}$ Zhang & Xu (2001), Li et al. (2006). In that sense it is possible to control independently the active and reactive power, adjusting the values of φ and V_c respectively Diaz et al. (2007). However, the VSI is a nonlinear double input double output coupled control system Zhang & Xu (2001). So the system cannot be easily controlled through conventional feedback controllers with fixed-gain. In addition, the power converter has important variations on its principal parameters, so, classical feedback controllers cannot compensate variations in the parameters of the system, and cannot be adapted to changes in the environment easily Gounden et al. (2009). Therefore, nonlinear controller appears as a possibility to control reactive and active power. A nonlinear fuzzy controller can work easily and directly with nonlinear systems and system that does not have constant parameters at the whole range of operating points, like the solid state converters. The fuzzy controllers do not use the parameters of the plant for their design Diaz et al. (2007), BABUSKA (2009). Then, fuzzy controllers may be used to control the active and reactive power flow and assure the MPPT by matching the impedance seen from the DC-DC converter under environmental changes.
The conversion stage is also composed by a step-up line-frequency coupling transformer and a low pass sine wave filter, designed to reduce the perturbation on the distribution system due to high-frequency switching harmonics generated by PWM control Xue et al. (2004), Kjaer et al. (2005), Molina & Mercado (2008).

3. MPPT algorithm

The slope of P-I curve (dP/dI) shown in figure 4 is positive on the left side of the maximum power point (MPP), negative on the right side of MPP and zero at MPP ($dP/dI = 0$). Based on that characteristic, the MPPT algorithm can be indicated as:

$$if\ dP/dI > 0;\ left\ of\ MPP,\ Then\ I\ must\ be\ increased.$$

$$if\ dP/dI = 0;\ at\ MPP,\ Then\ I\ must\ remain\ constant. \tag{13}$$

$$if\ dP/dI < 0;\ rigth\ of\ MPP,\ Then\ I\ must\ be\ decreased.$$

Adjusting the current at the PVG it is possible to track the maximum power point (MPP). The current at the DC side I_{dc} of the inverter is related to the ac current $i_{ac}(t)$ by the equation (14).

$$I_{dc} = Si_{ac}(t) \tag{14}$$

$$S = m\sin(\omega t + \varphi) \tag{15}$$

S is the rectangle switching function whose AC fundamental component is expressed in (15) Li et al. (2006). Besides the PV current I is related to DC current I_{dc} by (16) Erickson & Maksimovic (2000).

$$I = \frac{I_{dc}}{(1-D)} \tag{16}$$

$$I = \frac{m}{(1-D)}\frac{V_c}{X}\frac{\sin(2\varphi)}{2} \tag{17}$$

The PV current I depends of the duty cycle D at the first conversion stage, the modulation index m and the phase shift φ as can be seen in (17). Regarding a regulated DC voltage I depends mainly of the angle φ like the active power. So, the MPP can be obtained by adjusting the angle φ taking into account that m and D are imposed by the V_{dc} control and reactive power control respectively.
Taking into account that the power generated depends on solar irradiance and temperature as is shown in figure 4. It is desirable that if the system is close to the MPP the angle φ change a few. But if the system is far from the MPP the angle must change a lot.

4. Fuzzy MPPT algorithm

A fuzzy logic controller can easily incorporate all the qualitative knowledge above mentioned and summarized in (13) about the behavior of the system required to perform the MPPT. The fuzzy control also has the advantage to be robust and relatively simple to design, since it does not require the knowledge of the exact model Zeng & Liu (2009), Gounden et al. (2009), Larbes et al. (2009). A Mamdani fuzzy logic controller has been proposed to perform the MPPT, this kind of controller are usually used in feedback control mode, because they are computationally simple, present low sensibility to noise in the input (what is important in power system), and can easily represent the knowledge about the control action BABUSKA (2009). The knowledge is represented by means of rules in the form if-then and synthesized in form of an input-output mapping between the antecedent and the consequent variables BABUSKA (2009).

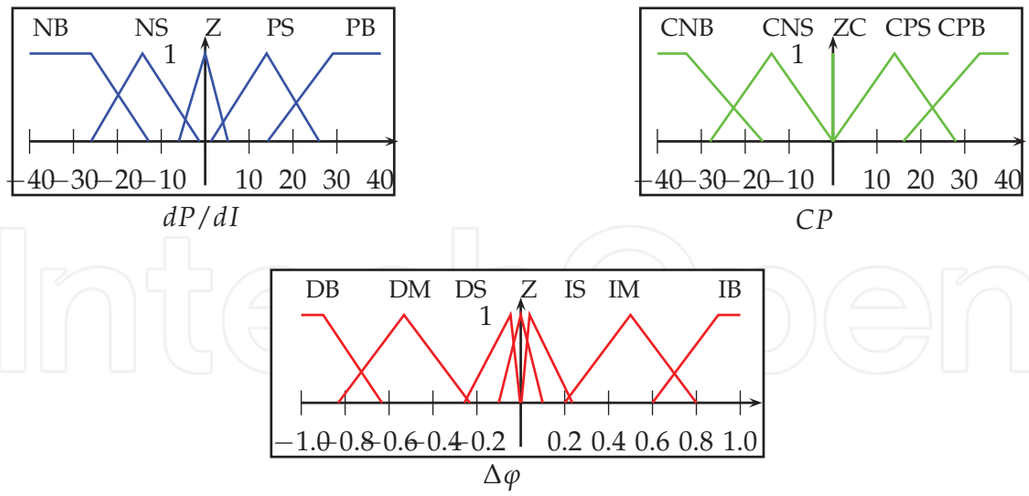

Fig. 8. FLC membership function for dP/dI, CP and $\Delta\varphi$.

A PD fuzzy logic controller (FLC) has been proposed in order to synthesize the MPPT algorithm. The inputs are the slope of the curve P-I (dP/dI) which shows the actual operation point, and the change of the power CP which expresses the moving direction of this point. In samples time $k = 1.4ms$. the inputs variables are defines as follow:

$$\frac{dP}{dI} = \frac{\Delta P}{\Delta I} = \frac{P(k) - P(k-1)}{I(k) - I(k-1)} \tag{18}$$

$$CP = \Delta P = P(k) - P(k-1) \tag{19}$$

The control rules are indicated in Table 2. Where (dP/dI) and CP are the inputs and the change in the phase shift $\Delta\varphi$ is the output. The membership function of the two input variables and the control action $\Delta\varphi$ are triangular and trapezoidal membership functions because of they are computationally simpler in figure 8 BABUSKA (2009). The membership functions were tuned searching the minimum error in steady state and the minimum oscillation in transitory state by trial and error method using the toolbox FIS of MATLAB. The input and output membership function are shown in figure 8 BABUSKA (2009).

4.1 Improvement of the MPPT by means of a fuzzy I_{sc} estimator

To avoid small current increments at high solar irradiance level and slow response of the MPPT, or high increments of the current at low irradiance level, that may cause high oscillations around the MPP, it is desirable a smaller step size of $\Delta\varphi$ under low irradiance,

CP dP/dI	CNB	CNS	ZC	CPS	CPV
NB	IB	IB	IB	IB	IM
NS	IM	IP	IP	Z	Z
Z	IP	Z	Z	Z	DP
PS	IM	IP	IP	Z	Z
PB	DN	DB	DB	DB	DB

Table 2. Rule Base FLC

and a higher step size of $\Delta\varphi$ under high irradiance. The step size of $\Delta\varphi$ might be weighted by the I_{sc} under different solar irradiance conditions. However, it is difficult to know in advance I_{sc} for all solar irradiance range and temperatures to weight the step size. To obtain the I_{sc} the PV generator should be disconnected from the system and by a short circuit in the generator the I_{sc} can be measured. A problem with this procedure is that available energy is wasted when the generator is disconnected from the system.

Figure 4, shows that the slope (dP/dI) for different levels of irradiance are similar in relation with the gap between the operating point and MPP location, where the gap depends on I_{sc}. Figure 9 shows different surfaces obtained by plotting the dP/dI values (under irradiance levels of $1000W/m^2$, $750W/m^2$ and $500W/m^2$) versus the normalized PV current I/I_{sc} and temperature. The figures are similar and they cannot be distinguished. Therefore, the curves under different weather conditions could be represented by an unique nonlinear model.

The nonlinear curves in figure 9 can be approximated by using a Takagi-Sugeno (TS) fuzzy model BABUSKA (2009). A TS fuzzy model can represent the nonlinear function as a smoothed piece-wise linear approximation as shown in figure 10. TS fuzzy model uses crisp functions of the antecedent variable at the consequents rather than fuzzy preposition like in FLC BABUSKA (2009). Hence, the model can be seen as a combination of linguistic and mathematical regression modeling in the sense that the antecedents describe fuzzy regions in the input space in which the consequent functions are valid BABUSKA (2009).

The TS model is obtained by means of fuzzy clustering algorithms that are used to partition an input-output data base into groups of similar objects. The term ”similarity” should be understood as mathematical similarity, it is often defined by means of a distance norm from a data vector to some prototypical object or center of cluster. The centers of clusters are usually unknown a priori, they are obtained by the clustering algorithms simultaneously with the partitioning of the data. The concept of graded membership is used to represent the degree at which a given data is similar to some center of cluster. Based on the similarity, the data can be clustered such that the data within a cluster are as similar as possible, then a cluster is a group of objects that are more similar to one another than to members of other clusters. The prototypes may be vectors of the same dimension as the data objects, but they can also be defined as ”higher-level” geometrical objects, such as linear or nonlinear subspaces or functions. Fuzzy clustering methods, allow the objects to belong to several clusters simultaneously, with different degrees of membership between 0 and 1 indicating their partial membership. That provides interpolation between clusters, what allow to approximate the nonlinear function BABUSKA (2009).

A clustering algorithm was used for the automatic generation of fuzzy models. The algorithm

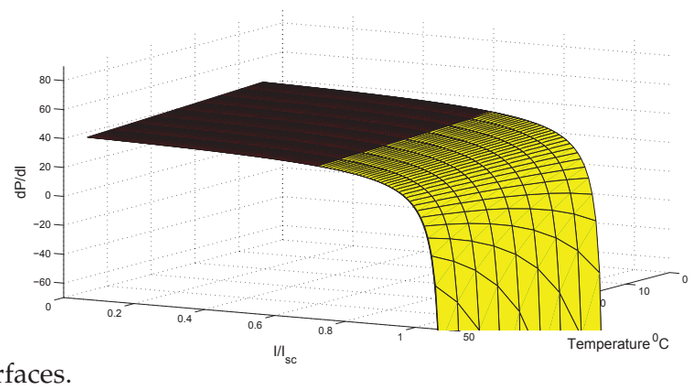

Fig. 9. dP/dI Surfaces.

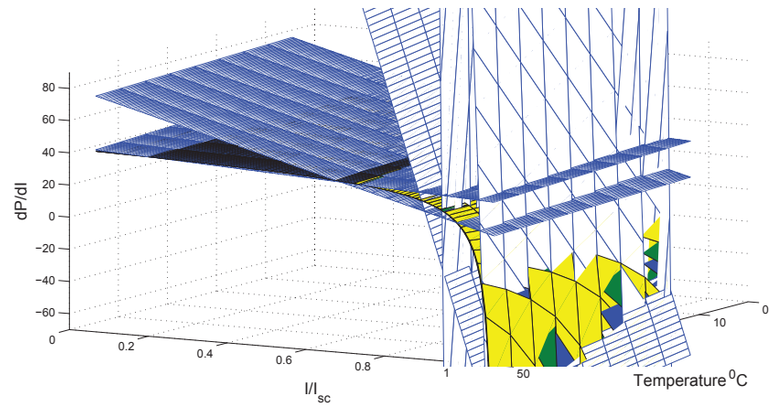

Fig. 10. Piece-wise linear approximation.

is based on optimization of the basic c-means objective function as exposed in BABUSKA (2009). The data base used to perform the algorithm is composed by the inputs dP/dI and temperature $Temp$, and the output of the model which is the normalized current I/I_{sc}. The data base is obtained from the PV generator model exposed before under variations of iradiance and temperature. Each obtained cluster is represented by one rule in the Takagi-Sugeno model.
The data base were partitioned into five clusters. Figure 10 shows the five local linear models obtained through clustering. Figure 11 shows the corresponding fuzzy partition of the consequents dP/dI and T. The parameters of the local linear models of each rule were obtained by least-squares estimation BABUSKA (2009). The TS rule base obtained is summarized as follow:

1. **If** dP/dI is A_{11} **and** $Temp$ is A_{12} **then**
   $I/I_{sc}(k) = 1.73 \cdot 10^{-3}u_1 - 4.21 \cdot 10^{-3}u_2 + 9.16 \cdot 10^{-1}$

2. **If** dP/dI is A_{21} **and** $Temp$ is A_{22} **then**
   $I/I_{sc}(k) = 2.50 \cdot 10^{-4}u_1 - 6.49 \cdot 10^{-4}u_2 + 9.97 \cdot 10^{-1}$

3. **If** dP/dI is A_{31} **and** $Temp$ is A_{32} **then**
   $I/I_{sc}(k) = -3.97 \cdot 10^{-3}u_1 + 2.97 \cdot 10^{-4}u_2 + 9.29 \cdot 10^{-1}$

4. **If** dP/dI is A_{41} **and** $Temp$ is A_{42} **then**
   $I/I_{sc}(k) = -3.52 \cdot 10^{-2}u_1 - 3.58 \cdot 10^{-3}u_2 + 1.90 \cdot 10^{0}$

5. **If** dP/dI is A_{51} **and** $Temp$ is A_{52} **then**
   $I/I_{sc}(k) = -1.20 \cdot 10^{-1}u_1 - 1.88 \cdot 10^{-2}u_2 + 5.31 \cdot 10^{0}$

Since, the PV current can be measured, it is possible to estimate the short-circuit current I_{sce} without disconnecting the PVG and measuring the short-circuit current. Figure 12 shows a comparison between the estimated short circuit current I_{sce} and the expected short circuit current I_{sc}. The percentile variance accounted for (VAF) between the I_{sc} and I_{sce} (formula 20) was used as a performance index of the TS fuzzy model where $VAF = 96.13\%$.

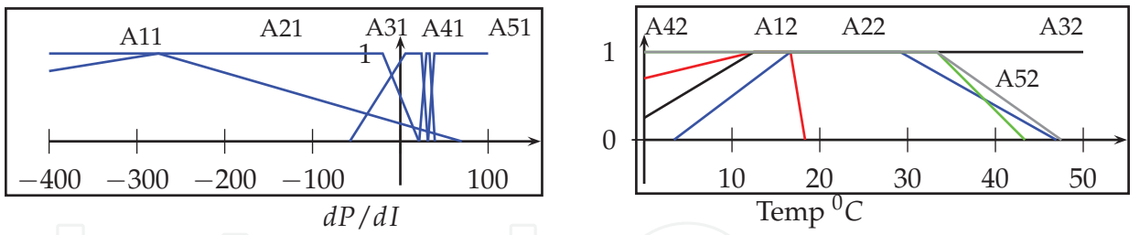

Fig. 11. TS fuzzy model input membership functions

$$VAF = 100\% \left[1 - \frac{var(I_{sc} - I_{sce})}{var\,(I_{sc})}\right] \tag{20}$$

The estimated I_{sce} weights the output of the (FLC) which allows adjust the step-size under different solar irradiance and then assure a step-size $\Delta\varphi$ proportional to the irradiance level. Another problem to solve is the operation of the system under solar irradiance decrements. When the solar irradiance deceases drastically the system operates in the right side of the MPP and hence the voltage on the PVG and the voltage V_{dc} become zero due to the relation given by (9). That may cause instability in the system since the condition for a normal operation of the system ($Vdc > Vs$) is not satisfied. Hence, the load should be decreased and the inverter should be turned off. To do that an additional crisp function has been added to the MPPT algorithm, it has the main function of reduce the angle φ to a half of its value when the PVG voltage decreases below 20V.

The fuzzy controllers are also composed of dynamic pre and post-filters the pre-filter used is an approximation of the derivative effect in the domain of discrete time, this approximation is often used and well accepted for computational implementation, the propose of the derivative effect is obtain a fast response to perturbations. To improve the precision in steady state was used an integrator as dynamic pos-filter in the output of the fuzzy controller Diaz et al. (2007), BABUSKA (2009).

4.2 Reactive power control

Since the inverter would be connected to power grid, the standards given by the utility companies must be obeyed (The power converter in a GCPV must have high conversion efficiency and a power factor exceeding 90% for wide operating range, while maintaining current harmonics THD less than 5%) Kjaer et al. (2005), Eltawil & Zhao (2010). The reactive power flow can be regulated by adjusting the AC voltage generated by the converter V_c as

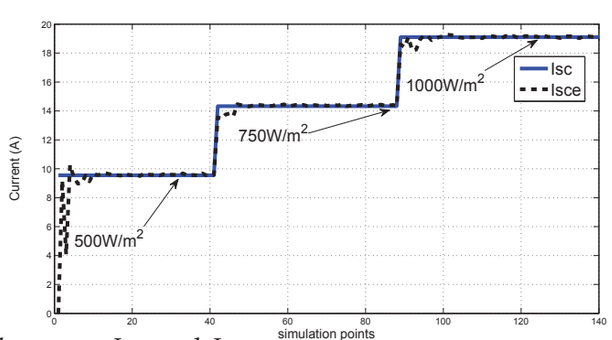

Fig. 12. Comparison between I_{sce} and I_{sc}.

ΔeQ / eQ	CNB	CNS	ZC	CPS	CPV
PB	Z	IS	IS	IM	IG
PS	DS	Z	IS	IS	IM
Z	DS	Z	Z	Z	IS
NS	DM	DS	DS	Z	IS
NB	DB	DM	DS	DS	Z

Table 3. Rule Base FCQ

is shown in (12). The V_c amplitude is regulate mainly by the modulation index m which is controlled by the SPWM signal. A Mamdani fuzzy controller has been designed to regulate the reactive power flow close to zero and deal with the nonlinear behavior.
The proposed controller is a kind of Fuzzy PD controller in counterpart of linear Proportional Derivative controllers BABUSKA (2009). The rule base of the the FCQ (Fuzzy Control of Q) has two inputs as antecedents; the error (eQ), and the error change (ΔeQ), In order to obtain a derivative effect. The output of the fuzzy inference system is the incremental variable (Δm). The rule base of FCQ is summarized in table 3. The FCQ was tuned in MATLAB using the fuzzy inference system toolbox. Dynamic pre and post-filters were also used on this controller.

5. Simulation results

The GCPVS was tested by simulation in the SimPowerSystem toolbox of MATLAB. The system is schematized in figure 5.
The simulation results in figure 13 show that the MPPT is achieved under different solar irradiance at 25^0C in the cell. The converter has a efficiency of 97%, and a settling time around $150ms$. The reactive power is also compensated by remaining it close to zero, then the power factor is close to one in steady state as shown in figure 14.
The TS fuzzy system became an efficient tool to estimate the short circuit current without disconnect the system. The estimator can be used in simpler MPPT methods like the short circuit current method, without having to shutdown the system in order to measure the short circuit current.

6. Short circuit current method

The P-I curves of the PV generator suggest a linear relation between the open short-circuit current (I_{sc}) and the maximum power point current (I_{MPP}) at different irradiance and temperature conditions A. Yafaoui (2009), Mutoh et al. (2006). This relation can be described by:

$$I_{MPP} = kI_{sc} \quad k < 1 \tag{21}$$

The value of the constant K depends on characteristics of the PV generator, but a commonly used value is 90% Mutoh et al. (2006). The short circuit current method is a very simple MPPT method, the PV current is compared with a constant reference current that corresponds to the I_{MPP}. The error signal can be used in simple controllers with integral action to eliminate the error in steady state Tariq & Asghar (2005).
One of the main drawback of this method is that available energy is wasted when the load is disconnected from the PV generator to measure the (I_{sc}). The measurement of the (I_{sc})

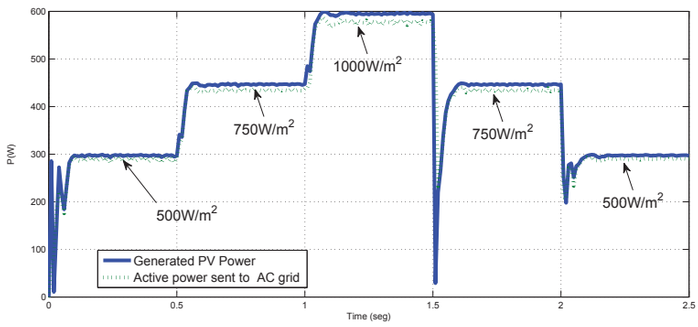

Fig. 13. Simulation results depicting the change of Power vs time.

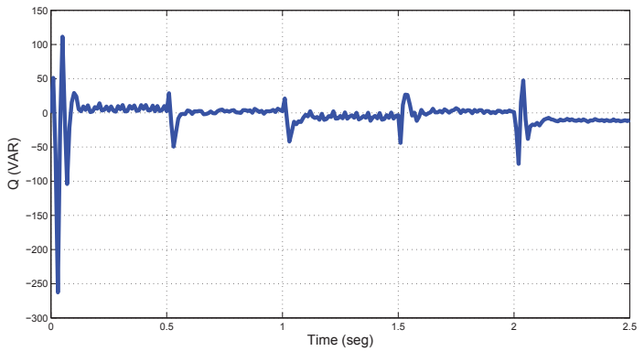

Fig. 14. Simulation results depicting the Reactive Power vs time.

during the operation of the system also increases the complexity of the circuit (I_{sc}). Moreover, the ambient conditions may change between the different measurements intervals and the PV generator conditions may vary A. Yafaoui (2009), Mutoh et al. (2006), Tariq & Asghar (2005). Those problems make this method less popular despite of its simplicity.
However, with the fuzzy short circuit estimator proposed before, the (I_{sc}) can be estimate without additional power power losses. The estimated short circuit current I_{sce} can be multiplied by the factor k in order to estimate the maximum power point current $(I_{MPPe}) = kI_{sce}$.
In order to verify this method a simple proportion integral (PI) controller has been designed. The reference of the controller is the I_{sce} multiplied by a factor $k = 0.88$. The simulation results in figure 15 show that the MPPT is achieved under different solar irradiance at 25^0C in the cell.

7. Conclusion

The MPPT algorithm can be easily synthesize by means of a fuzzy logic controller. The shape of the membership function of the fuzzy controllers can be adjusted in order to make the control action proportional to the gap between the operation point and the maximum power point. The increment of the conductance must be proportional to the solar irradiance to avoid high steps size under low irradiance or low step size under high irradiance, which may cause high oscillation around the maximum power point or high settling time under high solar irradiance. A good commitment has been achieved by weighting the step size of the MPPT algorithm by the short-circuit current.

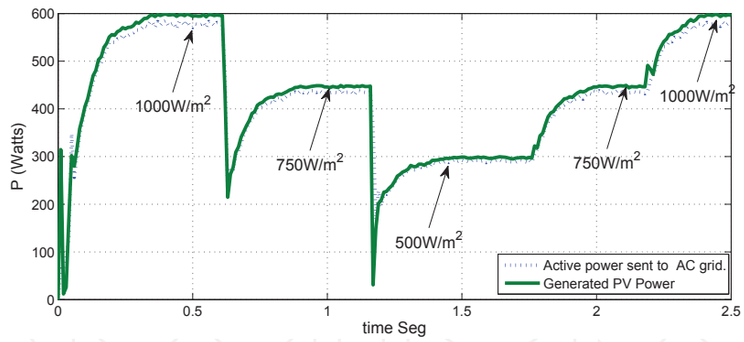

Fig. 15. Simulation results depicting the change of Power vs time with short circuit current method.

TS fuzzy system became an efficient tool to estimate the short circuit current without disconnecting the system. The estimator can be used in simpler MPPT methods like the short circuit current method, without having to shutdown the system in order to measure the short circuit current and then, overpass the main problem of this method. A similar strategy could be used to estimate the open circuit voltage improving the efficiency of this method since it will not be necessary to disconnect the panel from the PV system.

8. References

A. Yafaoui, B. Wu, R. C. (2009). Photovoltaic energy system part 2: System control technology, IEEE Canadian Review(61): 14–17.

Alonso-Martinez, J., Eloy-Garcia, J. & Arnaltes, S. (2009). Control of a three-phase grid-connected inverter for photovoltaic applications with a fuzzy mppt under unbalanced conditions, pp. 1 –7.

BABUSKA, R. (2009). *FUZZY AND NEURAL CONTROL DISC Course Lecture Notes*, Delft University of Technology.

Diaz, N., Barbosa, F. & Trujillo, C. (2007). Analysis and design of a nonlinear fuzzy controller applied to a vsc to control the active and reactive power flow, pp. 417 –422.

Eltawil, M. A. & Zhao, Z. (2010). Grid-connected photovoltaic power systems: Technical and potential problems–a review, *Renewable and Sustainable Energy Reviews* 14(1): 112 – 129.
URL: *http://www.sciencedirect.com/ science/ article/B6VMY -4WXB2C1- 2/2/ 409f2328d21fe83ec94cdc9198c79b76*

Erickson, R. W. & Maksimovic, D. (2000). Fundamentals of power electronics, second edition.

Gengyin, L., Ming, Z., Jie, H., Guangkai, L. & Haifeng, L. (2004). Power flow calculation of power systems incorporating vsc-hvdc, Vol. 2, pp. 1562 – 1566 Vol.2.

Gounden, N. A., Peter, S. A., Nallandula, H. & Krithiga, S. (2009). Fuzzy logic controller with mppt using line-commutated inverter for three-phase grid-connected photovoltaic systems, *Renewable Energy* 34(3): 909 – 915.
URL: *http://www.sciencedirect.com/ science/ article/ B6V4S -4SYKKV4- 3/2/ e53631c13f46e2efa5b430390e206d7a*

Hohm, D. & Ropp, M. (2000). Comparative study of maximum power point tracking algorithms using an experimental, programmable, maximum power point tracking test bed, pp. 1699 –1702.

Kim, I.-S., Kim, M.-B. & Youn, M.-J. (2006). New maximum power point tracker using sliding-mode observer for estimation of solar array current in the grid-connected photovoltaic system, *Industrial Electronics, IEEE Transactions on* 53(4): 1027 –1035.

Kjaer, S., Pedersen, J. & Blaabjerg, F. (2002). Power inverter topologies for photovoltaic modules-a review, Vol. 2, pp. 782 – 788 vol.2.

Kjaer, S., Pedersen, J. & Blaabjerg, F. (2005). A review of single-phase grid-connected inverters for photovoltaic modules, *Industry Applications, IEEE Transactions on* 41(5): 1292 – 1306.

Larbes, C., Cheikh, S. A., Obeidi, T. & Zerguerras, A. (2009). Genetic algorithms optimized fuzzy logic control for the maximum power point tracking in photovoltaic system, *Renewable Energy* 34(10): 2093 – 2100.
URL: *http://www.sciencedirect.com/ science/ article/ B6V4S -4VNCBXY- 1/2/ 48067b857bf072d0f7cc7c5fcd983d70*

Li, G., Li, G., Liang, H., Zhao, C. & Yin, M. (2006). Research on dynamic characteristics of vsc-hvdc system, p. 5 pp.

Molina, M. & Mercado, P. (2008). Modeling and control of grid-connected photovoltaic energy conversion system used as a dispersed generator, pp. 1 –8.

Mutoh, N., Ohno, M. & Inoue, T. (2006). A method for mppt control while searching for parameters corresponding to weather conditions for pv generation systems, *Industrial Electronics, IEEE Transactions on* 53(4): 1055 –1065.

Padiyar, K. & Prabhu, N. (2004). Modelling, control design and analysis of vsc based hvdc transmission systems, Vol. 1, pp. 774 – 779 Vol.1.

Patel, H. & Agarwal, V. (2006). Pv based distributed generation with compensation feature under unbalanced and non-linear load conditions for a 3- 003d5;, 4 wire system, pp. 322 –327.

Roman, E., Alonso, R., Ibanez, P., Elorduizapatarietxe, S. & Goitia, D. (2006). Intelligent pv module for grid-connected pv systems, *Industrial Electronics, IEEE Transactions on* 53(4): 1066 –1073.

Ruihua, S., Chao, Z., Ruomei, L. & Xiaoxin, Z. (2005). Vscs based hvdc and its control strategy, pp. 1 –6.

Sood, V. K. (2004). *HVDC and FACTS Controllers: Applications of Static Converters in Power Systems*, 1 edn, Springer.

Tariq, A. & Asghar, J. (2005). Development of an analog maximum power point tracker for photovoltaic panel, Vol. 1, pp. 251 –255.

Vandoorn, T., Renders, B., Belie, F. D., Meersman, B. & Vandevelde, L. (2009). A voltage-source inverter for microgrid applications with an inner current control loop and an outer voltage control loop.

Xiao, W., Lind, M., Dunford, W. & Capel, A. (2006). Real-time identification of optimal operating points in photovoltaic power systems, *Industrial Electronics, IEEE Transactions on* 53(4): 1017 –1026.

Xue, Y., Chang, L., Kjaer, S. B., Bordonau, J. & Shimizu, T. (2004). Topologies of single-phase inverters for small distributed power generators: an overview, *Power Electronics, IEEE Transactions on* 19(5): 1305 – 1314.

Zeng, G. & Liu, Q. (2009). An intelligent fuzzy method for mppt of photovoltaic arrays, Vol. 2, pp. 356 –359.

Zhang, G. & Xu, Z. (2001). Steady-state model for vsc based hvdc and its controller design, Vol. 3, pp. 1085 –1090 vol.3.

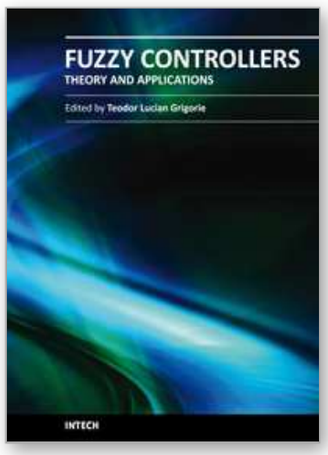

Fuzzy Controllers, Theory and Applications
Edited by Dr. Lucian Grigorie

ISBN 978-953-307-543-3
Hard cover, 368 pages
Publisher InTech
Published online 28, February, 2011
Published in print edition February, 2011

Trying to meet the requirements in the field, present book treats different fuzzy control architectures both in terms of the theoretical design and in terms of comparative validation studies in various applications, numerically simulated or experimentally developed. Through the subject matter and through the inter and multidisciplinary content, this book is addressed mainly to the researchers, doctoral students and students interested in developing new applications of intelligent control, but also to the people who want to become familiar with the control concepts based on fuzzy techniques. Bibliographic resources used to perform the work includes books and articles of present interest in the field, published in prestigious journals and publishing houses, and websites dedicated to various applications of fuzzy control. Its structure and the presented studies include the book in the category of those who make a direct connection between theoretical developments and practical applications, thereby constituting a real support for the specialists in artificial intelligence, modelling and control fields.

How to reference
In order to correctly reference this scholarly work, feel free to copy and paste the following:

Neson Diaz, Johann Hernández and Oscar Duarte (2011). Fuzzy Maximum Power Point Tracking Techniques Applied to a Grid-Connected Photovoltaic System, Fuzzy Controllers, Theory and Applications, Dr. Lucian Grigorie (Ed.), ISBN: 978-953-307-543-3, InTech, Available from: http://www.intechopen.com/books/fuzzy-controllers-theory-and-applications/fuzzy-maximum-power-point-tracking-techniques-applied-to-a-grid-connected-photovoltaic-system

INTECH
open science | open minds

InTech Europe
University Campus STeP Ri
Slavka Krautzeka 83/A
51000 Rijeka, Croatia
Phone: +385 (51) 770 447
Fax: +385 (51) 686 166
www.intechopen.com

InTech China
Unit 405, Office Block, Hotel Equatorial Shanghai
No.65, Yan An Road (West), Shanghai, 200040, China
中国上海市延安西路65号上海国际贵都大饭店办公楼405单元
Phone: +86-21-62489820
Fax: +86-21-62489821

© 2011 The Author(s). Licensee IntechOpen. This chapter is distributed under the terms of the Creative Commons Attribution-NonCommercial-ShareAlike-3.0 License, which permits use, distribution and reproduction for non-commercial purposes, provided the original is properly cited and derivative works building on this content are distributed under the same license.

IntechOpen

IntechOpen